



Harris, P., Boukley Hasan, W., Liu, L., Malkowsky, S., Beach, M., Armour, S., Tufvesson, F., & Edfors, O. (2018). Achievable rates and training overheads for a measured LOS massive MIMO channel. *IEEE Wireless Communications Letters*, 7(4), 594-597. [8274927].
<https://doi.org/10.1109/LWC.2018.2799863>

Peer reviewed version

Link to published version (if available):
[10.1109/LWC.2018.2799863](https://doi.org/10.1109/LWC.2018.2799863)

[Link to publication record in Explore Bristol Research](#)
PDF-document

This is the author accepted manuscript (AAM). The final published version (version of record) is available online via IEEE at <http://ieeexplore.ieee.org/document/8274927/references> . Please refer to any applicable terms of use of the publisher.

University of Bristol - Explore Bristol Research

General rights

This document is made available in accordance with publisher policies. Please cite only the published version using the reference above. Full terms of use are available:
<http://www.bristol.ac.uk/red/research-policy/pure/user-guides/ebr-terms/>

Achievable Rates and Training Overheads for a Measured LOS Massive MIMO Channel

Paul Harris, Wael Boukley Hasan, Liang Liu, Steffen Malkowsky, Mark Beach, Simon Armour, Fredrik Tufvesson and Ove Edfors

Abstract—This paper presents achievable uplink (UL) sum-rate predictions for a measured line-of-sight (LOS) massive multiple-input, multiple-output (MIMO) (MMIMO) scenario and illustrates the trade-off between spatial multiplexing performance and channel de-coherence rate for an increasing number of base station (BS) antennas. In addition, an orthogonal frequency division multiplexing (OFDM) case study is formed which considers the 90 % coherence time to evaluate the impact of MMIMO channel training overheads in high-speed LOS scenarios. It is shown that whilst 25 % of the achievable zero-forcing (ZF) sum-rate is lost when the resounding interval is increased by a factor of 4, the OFDM training overheads for a 100-antenna MMIMO BS using an LTE-like physical layer could be as low as 2 % for a terminal speed of 90 m/s.

Index Terms—Massive MIMO, Mobility, LOS, Testbed, Field Trials

I. INTRODUCTION

SINCE the conception of massive multiple-input, multiple-output (MIMO) (MMIMO) in [1], one aspect that has remained of interest is the operation of MMIMO under mobile conditions. Whilst the precision of decoding and precoding increases with a larger number of antennas, thereby improving spatial multiplexing performance, some techniques such as zero-forcing (ZF) are more sensitive to channel state information (CSI) error. The work in [2] analyses the impact of channel aging in MMIMO using the Jakes model and highlights the possibility of partial mitigation using channel prediction. It is also shown in [3] through simulations that user rates for MMIMO can drop radically for speeds as low as 10 km/h within urban environments. Similar results are presented for non-line-of-sight (NLOS) scenarios in [4] using measured data, but it is also shown that outdoor line-of-sight (LOS) conditions with minimal scattering can exhibit very high levels of stability. In strong LOS conditions with minimal scattering, a Doppler shift will occur between a moving terminal and static base station (BS) but the spread is minimal. Thus, orthogonal frequency division multiplexing (OFDM) systems will experience reduced inter-carrier interference (ICI) in these scenarios, even at high velocity, assuming the transmitters and receivers used can manage large carrier frequency offsets (CFOs). Furthermore, the increased coherence time that results from a low Doppler spread in LOS can allow more MMIMO

terminals to be trained for the same level of mobility, or an existing number to be supported at higher levels of mobility.

This paper serves as a companion paper to the work presented in [5]. Using data from the same measurement campaign, additional metrics are presented here to provide further insights on LOS MMIMO performance with terminal mobility. The authors believe these contributions will aid MMIMO system design and potentially serve to validate modeling assumptions. The remainder of the paper is structured as follows. In Section II, a brief recap of the MMIMO system and experiment configurations from [5] is given. The approaches for obtaining both the achievable uplink (UL) MMIMO sum-rate and the expected performance under channel aging are then presented in Section III. Section IV provides results for the sum-rate, depicts the trade-off between spatial multiplexing performance and coherence distance as the number of BS antennas M is increased, shows the impact of channel aging on detector performance and considers an application of the measured coherence time to an OFDM case study. The paper concludes in Section V.

II. MEASUREMENT SCENARIO

The results presented here use data acquired from the measurement campaign described in [5] where a 100-antenna real-time MMIMO BS is used to serve 8 user terminals in a LOS environment. The expected pilot signal to noise ratio (SNR) is in the range of 20–30 dB. All sum-rate results presented were obtained using the full 30 s mobile scenario, whereas the evaluation of coherence time is based upon the movement of car 2 through the 4 s scenario subset shown in Fig. 9 of [5]. For the latter it is ensured that the vehicle speed does not exceed 29 km/h such that the channel capture rate of 200 Hz (5 ms sounding period) meets the spatial Nyquist constraint of $\lambda/2$. For further details on the system or experiment, the reader should refer to the aforementioned paper.

III. CAPACITY EVALUATION

The aggregate uplink sum-rate is computed here for a given resource block b , time instance t and noise power N as

$$C_{\Delta}(b, t) = \sum_{i=1}^K \log_2 \left(1 + \frac{\left| \mathbf{h}_{i,b}^{norm}(t) \mathbf{w}_{i,b}^T(t - \Delta) \right|^2}{\sum_{j \neq i} \left| \mathbf{h}_{i,b}^{norm}(t) \mathbf{w}_{j,b}^T(t - \Delta) \right|^2 + N} \right) \quad (1)$$

where $\mathbf{h}_{i,b}^{norm}$ and $\mathbf{w}_{i,b}$ represent the channel and linear decoding vectors respectively for user i and frequency resource block b . $\mathbf{w}_{i,b}$ is derived using either ZF or matched filtering

P. Harris, Wael Boukley Hasan, M.A. Beach and S. Armour are with the Communication Systems & Networks (CSN) Group at the University of Bristol, U.K. Email: {paul.harris, wb14488, m.a.beach, simon.armour}@bristol.ac.uk

S. Malkowsky, O. Edfors, L. Liu and F. Tufvesson are with the Dept. of Electrical and Information Technology, Lund University, Sweden. Email: {firstname.lastname}@eit.lth.se

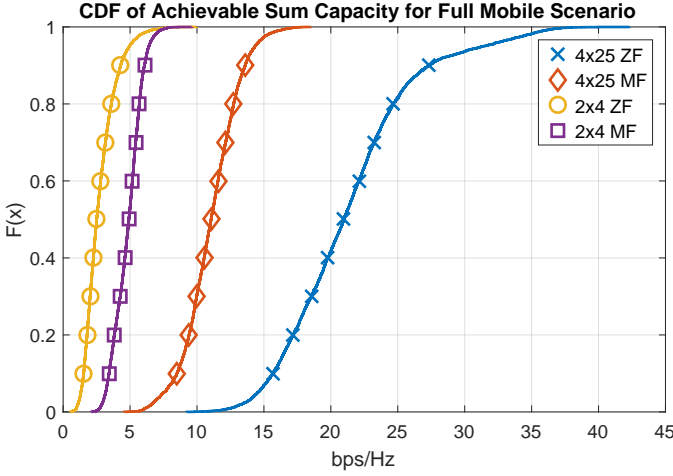


Fig. 1. Achievable sum-rate CDF for the full mobile scenario using ZF and MF for 100 and 8 BS antennas serving 4 dual-antenna USRPs clients (8 streams). Average SNR fixed to 30 dB

(MF) and Δ represents the time delay between CSI estimation and the application of the respective decoder weights. The calculation is thus based upon the Additive White Gaussian Noise (AWGN) capacity formula of [6] and a similar approach was used in [4]. To avoid noise power correlation and sum-rate inaccuracies, the decoding matrix \mathbf{W}_b is derived using the first CSI estimate and applied to the second when $\Delta = 0$. Applying a decoding matrix to the same channel matrix it was derived from is also impossible in a real system due to the fact that processing is not instantaneous and the CSI estimation will contain errors. For ZF, $\mathbf{W}_b = (\mathbf{H}_b \mathbf{H}_b^H)^{-1} \mathbf{H}_b^H$, and for MF, $\mathbf{W}_b = \mathbf{M}^{-1} \mathbf{H}_b^H$, where the latter division by the antenna dimension ensures the decoded MF power for a single user (no interference) is equal to 1 and matches ZF. The noise power N is then chosen to provide the desired average SNR for all users. In the cases where spectral efficiency is given per user, the median sum-rate across K active user vectors is taken unless otherwise specified.

A statistical measure was also calculated to evaluate the percentage of the achievable sum-rate one can expect to obtain with ageing decoder weights. Referred to as the expected sum-rate, it is defined as shown in (2) as the ratio of the achievable sum-rate given some channel resounding interval Δ to the achievable sum-rate when $\Delta = 0$.

$$\gamma(\Delta) = \mathbf{E} \left\{ \frac{C_\Delta(t)}{C(t)} \right\} \quad (2)$$

IV. RESULTS

A. Achievable Rate

As described in Section III, the decoder matrices are calculated using the channel matrix one sample (5 ms) prior to the channel matrix they are applied to in order to avoid noise summation and unrealistic sum-rate results. Fig. 1 and Fig. 2 show both the achievable sum-rate cumulative distribution function (CDF) and the results across time respectively over the full 30 second mobile scenario for the

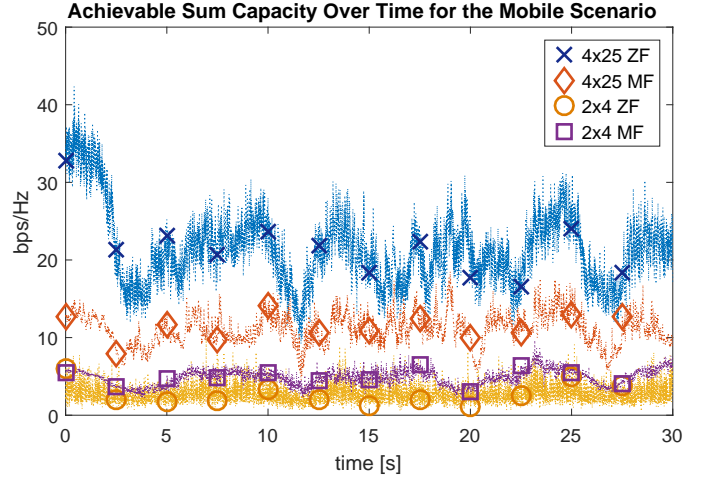


Fig. 2. Achievable sum-rate over time for the full mobile scenario using ZF and MF for 100 and 8 BS antennas serving 4 dual-antenna USRPs clients (8 streams). Average SNR fixed to 30 dB

4×25 and 2×4 BS array configurations serving 4 dual-antenna USRPs clients (8 streams). The average SNR was fixed to 30 dB. With the full 100 antenna configuration, ZF offers the best performance, providing a median achievable spectral efficiency of 21 bits/s/Hz and peaks in the 30–40 bits/s/Hz range. The median MF performance is a factor of two smaller at 11 bits/s/Hz, but exhibits less variance, spanning 5–18 bits/s/Hz compared to 9–43 bits/s/Hz for ZF. When the time domain representation is inspected (Fig. 2), it is possible to see the impact of terminal movement upon the achievable sum-rate. At the beginning of the scenario when the pedestrians and cars start to move, there is an obvious impact for the 100 antenna ZF case. Whilst static, the achievable sum-rate ranges between 30–40 bits/s/Hz, but after two seconds once movement has commenced, the sum-rate drops sharply by half and averages 20 bits/s/Hz for the remainder of the scenario. MF, whilst performing worse, experiences far less variance across the scenario, indicating the impact of channel aging is not as severe. In the 2×4 case, the ZF performance is very poor. The variance it exhibits around a mean value of 2.7 bits/s/Hz implies the equalization resulted in very low signal to interference plus noise ratio (SINR). Across all time samples and all users, the mean SINR following equalization using ZF was -6.8 dB, compared to -2.8 dB for MF. In such a case it is better to yield the full coherent beamforming gain of M provided by MF and tolerate the interference, but the result is still not ideal, and the benefits of large M for linear detection can clearly be seen.

B. The Impact of Antennas on CSI Update Rates

By further inspecting the temporal correlation results obtained in [5], some insight can be gained on the trend of decorrelation with relation to the number of BS antennas and terminal distance moved. As previously shown in [5], the elevation dimension did not impact the rate of decorrelation in this LOS scenario; it was primarily dictated by the azimuth resolution. Thus, Fig. 3 shows the terminal distance moved for a spatial channel decorrelation of 10% as a function of the

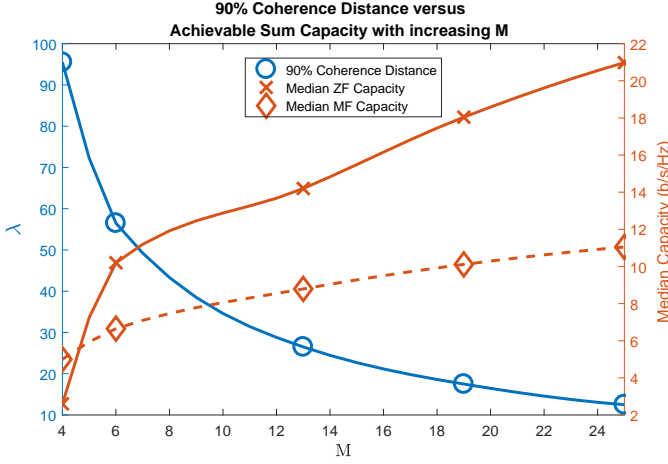


Fig. 3. Terminal distance moved in wavelengths for 10% spatial decorrelation versus median achievable sum-rate. M represents the number of elements in the azimuth for the $4 \times M$ array.

number of BS antennas in the azimuth only. For comparison purposes, the median achievable UL sum-rate results have been plotted on a second axis, and a cubic interpolation has also been applied to the data points for both so that the trend can be visualized. For the achievable UL sum-rate, the number of antennas M refers to the azimuth dimension, but all four rows of elevation were used for MIMO decoding. As the number of BS antennas grow, it is clear that a trade-off must be made. On the one hand, increasing the number of antennas creates a greater level of pairwise orthogonality between the user channel vectors and thus increases the achievable UL sum-rate, but the corresponding reduction in coherence time also increases the channel training requirements for each user further explaining the observations in [5].

C. Expected Rate

In Fig. 4, the expected sum-rate is shown for the 2×4 and 4×25 array configurations using both ZF and MF. The sensitivity of achievable performance to channel estimation error for MF is not as severe as for ZF, but the lack of interference mitigation typically results in a lower sum-rate when the user channel vectors are highly correlated. For 8 antennas, increasing Δ up to 20 ms results in an initial drop in the expected sum-rate of approximately 10 %, but the performance reduction then plateaus. For the 100 antenna case this plateau occurs 5 % lower, but the sum-rate reduction trend is very similar. This indicates the impact of channel aging on the achievable MF sum-rate is limited in this case, even with large M . ZF performance suffers more from channel estimation error as it results in the inaccurate placement of nulls. Thus, the interference is not mitigated as effectively and the SINR reduces for each user terminal. As with large M the nulls become more focused, the sensitivity of ZF performance to user mobility worsens, and it may be necessary to use a higher correlation percentage when calculating a suitable coherence time. The impact of M upon ZF performance with an increasing resounding interval is clearly shown in Fig. 4. It can be seen that the exponential decay of expected sum-rate

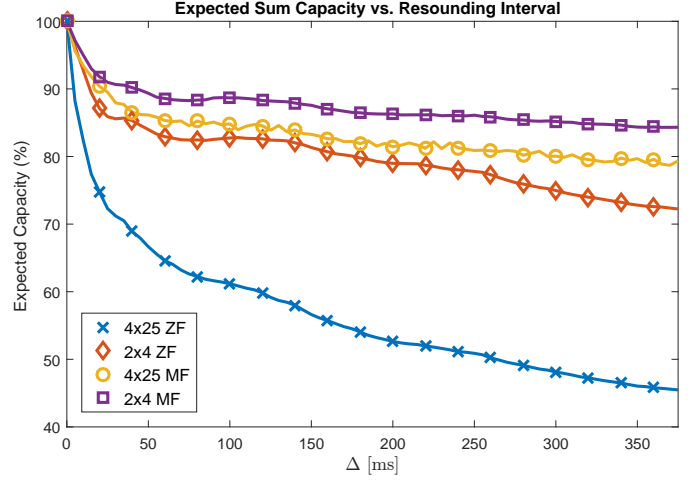


Fig. 4. Expected sum-rate for ZF and MF versus channel resounding interval Δ across the full 30 s mobile scenario

after increasing Δ by only tens of milliseconds is far more extreme for the 4×25 case, losing 25 % of the sum-rate for $\Delta = 20$ ms. This equates to a displacement in wavelength of only 2λ (16.2 cm).

D. Case Study on Outdoor LOS Training Overheads

A case study was formed to evaluate the impact the aforementioned outdoor LOS channel coherence results would have upon training overhead in an long-term evolution (LTE)-spec OFDM MMIMO system. As channel prediction techniques such as those in [2] are not included here, it should be considered a worst case. The coherence interval, τ_c , defines the number of samples available within a time and frequency coherent period for pilot and data transmission. In extreme cases where τ_c is very small, the number of users it is possible to train will be severely reduced and the training overhead will reduce the available samples, limiting data transmission. To formulate this case study, the background definitions for OFDM coherence intervals and first-order coherence bandwidth approximations described in [7] are called upon. The coherence bandwidth B_c can be expressed in terms of OFDM subcarriers as a frequency smoothness interval N_{smooth} , defined as

$$N_{smooth} = \left\lfloor \frac{B_c}{B_s} \right\rfloor \quad (3)$$

where B_s is the subcarrier bandwidth. Assuming a first order approximation for B_c of 300 kHz, appropriate for outdoor environments, and the 15 kHz subcarrier width of LTE, N_{smooth} is 20. Similarly, T_c can be expressed as a number of OFDM symbols in a coherence slot as

$$N_{slot} = \left\lfloor \frac{T_c}{T_s} \right\rfloor \quad (4)$$

where T_s is the OFDM symbol duration and T_c is the channel coherence time. For an LTE OFDM system, T_s is typically 71.4 μ s, and this is the value used here. T_c was measured in [5] for this LOS scenario to be 125 ms for 90 % coherence at 29 km/h. Therefore, at an upper extreme of 100 m/s, T_c would become approximately 10 ms for 90 % coherence, and

the value for N_{slot} and τ_c would become 140 and 2800 respectively. As $\tau_c \gg M$ in this high mobility case, it is assumed that it will always be possible to train $M/2$ users in this study. Theoretically, this is the optimum number of users to serve when $\tau_c \gg M$ and the SNR is high as described in [7]. It is also assumed that all users in the system will use the full 20 MHz system bandwidth corresponding to 1200 subcarriers. With an N_{smooth} of 20, one OFDM pilot symbol permits 20 users to obtain full CSI. Thus, the number of symbols required for training N_{train} is fixed at 3 and the training overhead in % can be expressed as

$$T_{OH} = \frac{N_{train}}{N_{slot}} \times 100 \quad (5)$$

Fig. 5 shows the channel training overhead T_{OH} against terminal velocity for the LOS scenario studied here using different array sizes. It shows that even in the most extreme case using 100 antennas with the terminal moving at 100 m/s in parallel to the azimuth of the BS array, typical of a high-speed train scenario, the channel training overhead is just a little over 2 %. With more realistic vehicular speeds of up to 30 m/s, it is around 0.5 %. These results indicate that outdoor environments with a strong LOS characteristic can be highly stable for MMIMO systems and a far larger azimuth dimension could be permitted in this case. By increasing the azimuth dimension and thereby the LOS angular resolution, spatial selectivity would be further improved and more users could be served effectively in the same time-frequency resource. T_c would also reduce, but the above results suggest that there could be a large margin in this type of scenario, and it could be desirable to increase the training percentage of the coherence interval to obtain the MMIMO benefits and increase the number of connected devices in the spatial domain. As an example, this would bode well for the long-range rural applications Facebook are targeting with Project Aries in [8], as the 96-antenna system has a 2×48 azimuth dominated configuration. Finally, when following the MMIMO system design process shown in [9], the improved channel stability encountered within these LOS scenarios would relax the time division duplex (TDD) MMIMO precoding turnaround constraints and reduce the cost of commercial system development.

V. CONCLUSIONS

This paper has presented results for the achievable MMIMO sum-rate, the impact of channel aging and the required training overheads for a 100-antenna MMIMO OFDM system in a measured LOS scenario with mobility. The results serve as accompanying material for the work originally presented in [5]. When serving 8 single antenna user terminals, it was shown that a median UL sum-rate of 20 bits/s/Hz and 10 bits/s/Hz could be achieved for ZF and MF respectively. Furthermore, 25 % of the achievable UL ZF sum-rate was lost by increasing the resounding interval by a factor of 4. The channel de-coherence in that case was measured to be just 3 %, indicating how sensitive ZF can be to channel aging. Finally, the training overhead for the LOS scenario considered assuming an LTE-like OFDM physical layer was calculated to be 2 % at 90 m/s. This implies a large margin could be

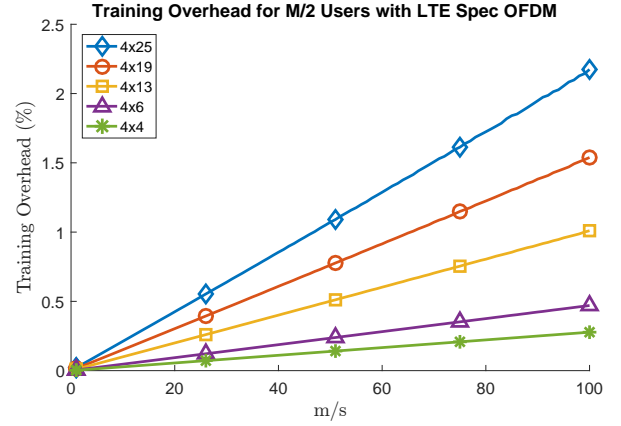


Fig. 5. The percentage of OFDM symbols that will be required to train $M/2$ (50) users at different speeds in the aforementioned LOS scenario. Array configurations of varying azimuth size considered using 10 % decorrelation as a threshold for T_c , 300 kHz as a first order approximation of B_c and an LTE OFDM symbol duration of 71.4 μ s

available in such scenarios for a MMIMO system to train more users, support greater terminal velocity and relax the precoding turn-around latency constraints in a TDD configuration.

ACKNOWLEDGMENT

The authors acknowledge and thank all academic staff and post graduate students involved at both Lund University and the University of Bristol who contributed to the measurement trial operations. They also acknowledge the financial support of the Engineering and Physical Sciences Research Council (EPSRC) Centre for Doctoral Training (CDT) in Communications (EP/I028153/1), NEC and National Instruments (NI).

REFERENCES

- [1] T. L. Marzetta, "Noncooperative cellular wireless with unlimited Numbers of base station antennas," *IEEE Transactions on Wireless Communications*, vol. 9, no. 11, pp. 3590–3600, Nov 2010.
- [2] K. T. Truong and R. W. H. Jr., "Effects of Channel Aging in Massive MIMO Systems," *CoRR*, vol. abs/1305.6151, 2013. [Online]. Available: <http://arxiv.org/abs/1305.6151>
- [3] P. Kela, X. Gelabert, J. Turkka, M. Costa, K. Heiska, K. Leppänen, and C. Qvarfordt, "Supporting mobility in 5G: A comparison between massive MIMO and continuous ultra dense networks," in *2016 IEEE International Conference on Communications (ICC)*, May 2016, Kuala Lumpur, Malaysia.
- [4] C. Shepard, J. Ding, R. E. Guerra, and L. Zhong, "Understanding real many-antenna MU-MIMO channels," in *2016 50th Asilomar Conference on Signals, Systems and Computers*, Nov 2016, pp. 461–467.
- [5] P. Harris, S. Malkowsky, J. Vieira, E. Bengtsson, F. Tufvesson, W. B. Hasan, L. Liu, M. Beach, S. Armour, and O. Edfors, "Performance Characterization of a Real-Time Massive MIMO System With LOS Mobile Channels," *IEEE Journal on Selected Areas in Communications*, vol. 35, no. 6, pp. 1244–1253, June 2017.
- [6] C. E. Shannon, "A mathematical theory of communication," *The Bell System Technical Journal*, vol. 27, no. 4, pp. 623–656, Oct 1948.
- [7] T. L. Marzetta, E. G. Larsson, H. Yang, and H. Q. Ngo, *Fundamentals of Massive MIMO*. Cambridge University Press, 2016.
- [8] "Facebook Project Aries," 2016. [Online]. Available: <https://code.facebook.com/posts/1072680049445290/introducing-facebook-s-new-terrestrial-connectivity-systems-terragraph-and-project-aries/>
- [9] S. Malkowsky, J. Vieira, L. Liu, P. Harris, K. Nieman, N. Kundargi, I. C. Wong, F. Tufvesson, V. Öwall, and O. Edfors, "The World's First Real-Time Testbed for Massive MIMO: Design, Implementation, and Validation," *IEEE Access*, vol. 5, pp. 9073–9088, 2017.